

In-situ RHEED Analysis of Atomic Layer Deposition

R.G. Bankras, J. Holleman, J. Schmitz
MESA⁺ Institute of Nanotechnology,
Chair of Semiconductor Components, University of Twente
P.O. Box 217, 7500 AE Enschede, The Netherlands
phone: +31 (0)53-489 2729, fax: +31 (0)53-489 1034
e-mail: r.g.bankras@utwente.nl

Abstract— Recent efforts on growth modeling of the atomic layer deposition process emphasized the need of an accurate understanding of the process, especially for the initial stage of the deposition. This paper presents results obtained from in-situ RHEED measurements during atomic layer deposition of Al₂O₃ on Si(001), using Al(CH₃)₃ and H₂O as precursors. The results show the expected decrease in reflected intensity on deposition of aluminum atoms. Also, a recovery of intensity was observed on exposure to H₂O. This recovery is contributed to removal of methyl groups from the surface, resulting in an improvement of surface roughness. Finally, the intensity decay is analysed using a simple growth model.

Keywords— reflection high-energy electron diffraction (RHEED); atomic layer deposition (ALD); high-k gate dielectrics; aluminum oxide (Al₂O₃)

I. INTRODUCTION

One of the barriers in the continuing downscaling of transistors is the high leakage current through the MOS stack. The search for a new gate dielectric material, to replace the traditional SiO₂, has resulted in Hf-based oxides being the most promising candidates at the moment. Although dielectric constant and the leakage currents at progressing EOT values become acceptable, several interface related problems still have to be solved.

The replacement of the conventional thermally grown SiO₂ by a high- κ dielectric material was accompanied by the introduction of the atomic layer deposition (ALD) technique to front-end semiconductor manufacturing. Although leakage currents become acceptable at progressing equivalent oxide thickness (EOT), several interface-related problems remain unsolved. In the initial stage of the ALD process, a low nucleation rate due to a low reactive sticking of precursors with the silicon surface is the cause of growth inhibition. [1] Characterization of this part of the deposition process is usually ex-situ [2] and at best without a vacuum break. [3] In-situ monitoring of ALD with RHEED could provide direct growth information, contribute to growth model development and lead to improvement of device characteristics.

The ALD process of metal oxides is based on the sequential exposure to oxidizing and reducing precursor vapors. The precursor molecules, e.g. the reducing ones, saturate the surface by chemisorption. This process is limited by the amount of suitable, available and accessible bonding sites. A second precursor is used as an oxidizing agent, removing ligands of the first precursor molecules on the surface and creating new bonding sites for the first precursor. Successful layer-by-layer growth is achieved by sequential repetition of both steps and avoiding gas phase reactions between both precursors. The deposition rate, or growth-per-cycle, is considered to be constant during the bulk deposition of the layer.

Reflection high-energy electron diffraction (RHEED) is widely used for in-situ analysis of (crystalline) growth in pulsed laser deposition (PLD) [4] and molecular beam epitaxy (MBE) [5] systems. Several ALD layers have been studied by ex-situ RHEED [6, 7, 8], although only photographs of the diffraction patterns are presented. A beam of high energy electrons (5 - 35 keV) is reflected off the sample surface at grazing incident angles, usually 1 - 3° with respect to the wafer surface. The wavelength of the electrons (0.070 Å at 30 keV) is considerably smaller than the size of and the distance between the scattering centers, i.e. atoms on (or near) the surface. Therefore, atomic features play a role in the diffraction and reflection. Diffraction spots and intensity oscillations of the diffracted beam(s) yield information on the growth mechanism. [9] Intensity oscillations, observed during epitaxial growth, have been related to the sequential completion of monolayers. [10]

II. MODELING OF RHEED AND ALD PHYSICS

In a simple and commonly used deposition model, a finite area is considered to be covered with cubic blocks in a close-packed array. The building blocks represent single atoms, molecules, unit cells or another unit of the deposited material. A set of basic deposition rules is used to define the preferential form of the deposition, resulting in different growth modes. Calculation of the change in

RHEED intensity during an ALD process, requires simplification of the electron-surface interaction.

The electron wavelength is much smaller than the size of an atom. Therefore, the interaction of electrons with the surface atoms in RHEED analysis should be described using wave mechanics. The reciprocal of the electron wavelength is the amplitude of the wave vector $|\mathbf{k}| = 2\pi/\lambda$. The momentum transfer of the incident wave with vector \mathbf{k}_0 to an exit wave with vector \mathbf{k} , due to scattering on a surface atom (see figure 1), is $\mathbf{u} = (\mathbf{k} - \mathbf{k}_0)$. In elastic scattering, the amplitude of the exit wave vector is equal to the amplitude of the incident wave vector.

Incident electrons interact with the potential distribution of atoms at and near the surface. [11] In the Born approximation, i.e. single atom scattering, the scattering amplitude is proportional to the Fourier transform of the scattering object. [12] Summation over all scattering objects of interest, results in the scattering amplitude of electrons with the surface

$$A(\mathbf{u}) = \sum_{\mathbf{v}} f(E, \varphi) \cdot e^{-i \cdot \mathbf{u} \cdot \mathbf{v}}, \quad (1)$$

with scattering factor $f(E, \varphi)$ as function of electron energy E and scattering angle φ . This factor has been published in tabulated form for most elements in neutral and ionized state. [13] The real space vector \mathbf{v} describes the distance from an arbitrary origin to the scattering atoms and consists of in-plane and layer-to-layer components. The latter is $|\mathbf{v}_{\perp}| = n \cdot d$, with interlayer spacing d and n an integer. The momentum transfer can also be split in parallel \mathbf{u}_{\parallel} and perpendicular \mathbf{u}_{\perp} components. Neglecting the scattering due to lateral distribution of atoms [14] is allowed because of the large sampled area. Equation 1 then becomes

$$A(\mathbf{u}_{\parallel} = 0, \mathbf{u}_{\perp}) = \sum f(E, \varphi) \cdot e^{-i \cdot \mathbf{u}_{\perp} \cdot n \cdot d}. \quad (2)$$

Interference of waves is constructive when their phase (shift) difference is less than half the wavelength. Maximum constructive interference occurs where waves are exactly in phase. Combining Bragg's law with the wave vector amplitude, results in the momentum transfer for in-phase and out-of-phase conditions of electrons scattered from the top layer with electrons scattered from the underlying layer. The two conditions are set in equation 2, by substituting \mathbf{u}_{\perp} with $2\pi/d$ or π/d respectively. The RHEED intensity is finally calculated as the square modulus of the scattering amplitude $I(\mathbf{u}) = |A(\mathbf{u})|^2$.

In the solid-on-solid model, blocks are deposited directly on top of filled positions (see figure 1). The coverage of the n^{th} layer $S^{(n)}$ therefore depends on the coverage of the underlying layer $S^{(n-1)}$. Layer-by-layer growth

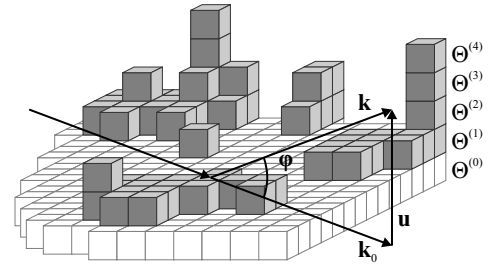


Fig. 1

SOLID-ON-SOLID SURFACE MODEL WITH ELECTRON SCATTERING VECTORS \mathbf{k} AND \mathbf{k}_0 , AND REFLECTION ANGLE φ . THE DEPOSITED LAYERS ARE $\Theta^{(n)}$ ON SUBSTRATE $\Theta^{(0)}$.

is modeled with rules which fill a layer completely before starting a new layer. Nucleation of islands can be modeled by a set of rules which prefer growth on top of deposited material, instead of filling uncovered substrate positions. The growth mode in an atomic layer deposition process depends on the deposited material, the used precursors, temperature and the type of substrate (termination). The ALD process of Al_2O_3 from TMA and H_2O on a H-passivated substrate has been identified to start with island formation.

The formation of islands by random deposition has been described using a discrete time model (ALD cycles), [15] similar to the birth-death time-domain models for epitaxial deposition. [14] In the latter model, the change in surface structure has been related to the electron scattering intensity of RHEED analysis, [16] although the scattering factor was simplified to unity. The inhibited growth is caused by the slow conversion of the initial surface passivation to the preferred (and required) OH-terminated surface. Thus, the growth per cycle $\Delta\Theta_j$ changes from a low rate during interface formation to a higher rate during deposition of the bulk. The average growth per cycle is calculated as a linear combination of both deposition rates,

$$\Delta\Theta_j = \Delta\Theta_{\text{Si}} \cdot S_{\text{Si}} + \Delta\Theta_{\text{AlO}_x} \cdot S_{\text{AlO}_x}, \quad (3)$$

where $\Delta\Theta_{\text{Si}}$ and $\Delta\Theta_{\text{AlO}_x}$ are the growth rate of Al_2O_3 on Si and AlO_x , respectively. [15] The sum of the uncovered surface fraction S_{Si} and deposited material (covered surface) S_{AlO_x} , is unity for every ALD cycle $j = 1 \dots J$. The surface fraction $S_j^{(n)}$ is the part of layer n which is not covered by layer $n + 1$. The new surface fractions $S_j^{(n)}$ of layers $n = 0 \dots N$ can be calculated using the growth per cycle in ALD cycle j .

The initial situation is an empty substrate $S_0^{(0)} = 1$, without deposited material $S_0^{(n)} = 0$ for $n > 0$ and the subsurface layers are fully covered by the top layer of the substrate $S_j^{(n)} = 0$ for $n < 0$. Including only scattering

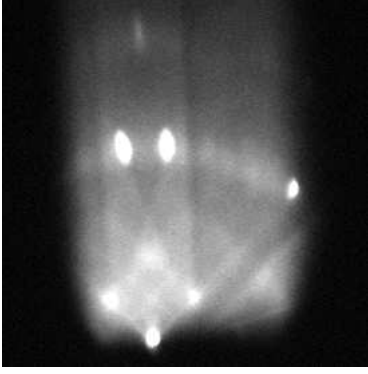


Fig. 2

ELECTRON DIFFRACTION PATTERN OF A BARE Si(001) SURFACE.

on blocks that form the top layer, equation 2 is changed to sum over all deposited layers

$$A_j = f_{\text{Si}} \cdot S_j^{(0)} + f_{\text{AlOx}} \cdot \sum_{n=1}^J S_j^{(n)} \cdot e^{-i \cdot \mathbf{u}_{\perp} \cdot n \cdot d}, \quad (4)$$

with their respective surface fractions $S_j^{(n)}$. Different scattering factors for the uncovered substrate f_{Si} and for the deposited material f_{AlOx} allows the model to differentiate between materials.

III. EXPERIMENTAL

A custom-designed reactor was realized to study the ALD growth of high- κ dielectrics. The reactor is turbo molecular pumped and contains a small process chamber of about 80 cm³, which can be tilted with respect to the RHEED system. The process chamber consists of a heated pedestal which supports the sample (bottom), a gas distribution block (wall) and a heated cover. Small slits in the process chamber allow in-situ RHEED analysis during deposition. The RHEED system is based on the high pressure RHEED setup used for PLD, [4] which can be used at relatively high process pressures (up to about 0.5 mbar).

Before deposition, 100 mm p-type Si(001) substrates have been cleaned of organic and metallic contamination using 100% HNO₃ and 69% boiling HNO₃, respectively. Native oxide was etched using a solution of 0.3% HF and 0.37% HCl in H₂O, resulting in a smooth H-terminated surface. After loading, the wafer was heated to the deposition temperature (300°C) at 10 mbar N₂ in 30 minutes. The two precursors, Al(CH₃)₃ and H₂O, are cooled to 18.0 and 15.0 °C, resulting in constant vapor pressures of about 19 and 11 mbar respectively. Transport of precursor to the deposition reactor is regulated by the difference between vapor pressure and reactor pressure, and is

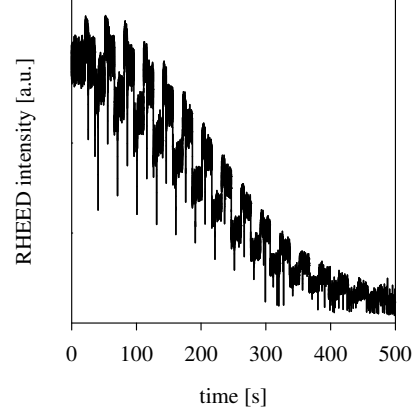


Fig. 3

DECAY OF RHEED INTENSITY DURING THE ALD PROCESS OF AL₂O₃.

restricted by a needle valve. Next, a 4-step deposition cycle, i.e. H₂O pulse, N₂ purge, TMA pulse, and N₂ purge, was repeated until the required thickness was deposited. The recipe times are reactor specific and can be increased for experimental purposes, within the limits of stability of the chemisorbed precursor.

A double differentially pumped STAIB Instrumente RH30DP electron source was used to generate a focused beam of 30 keV electrons. Diffraction conditions were achieved by tilting the sample with respect to the electron beam and visualized using a fluorescent (phosphor) screen. The diffraction pattern was recorded during deposition by a 10-bit CCD camera and frame grabber, at a speed of about 64 fps. The lateral and longitudinal intensity profiles of the specular reflected spot were stored, combined with the actual control signal of the precursor valves. Post-processing of the recorded information consisted of fitting (linear offset) Gaussian functions to the captured profiles, using a least squares optimization by Newton-Raphson iterations.

IV. RESULTS

Most of the diffraction pattern is shadowed by the narrow slits in the gas block. The number of visible diffraction spots depends on the alignment of electron beam and process chamber (sample), with respect to the fluorescent screen. Figure 3 shows the reduction in RHEED intensity (of the specular spot) for the first 20 ALD cycles.

Figure 4 shows the results of thickness measurements by XPS of the deposited layer, as determined from the Al 1p peak. The samples have been transferred to the XPS

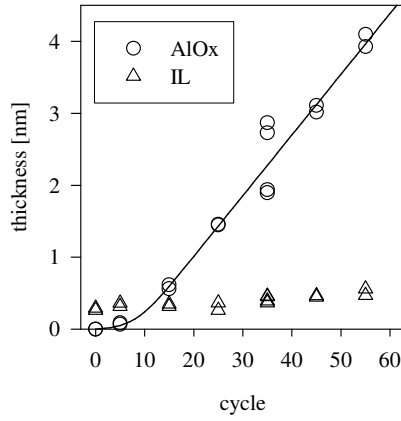


Fig. 4

THICKNESS MEASUREMENTS BY XPS (UNDER 0 AND 45°) OF THE Al_2O_3 AND INTERFACE LAYER AFTER SEVERAL ALD CYCLES. THE LINE REPRESENTS THE GROWTH CURVE FOR $\Delta\Theta_{\text{Si}} = 0.024$ AND $\Delta\Theta_{\text{AlOx}} = 0.393$.

without a vacuum break. A linear (least squares) fit of the measurement points of 15, 25, 45 and 55 cycles, results in a growth rate of $8.45 \cdot 10^{-2}$ nm/cycle. With the monolayer thickness as determined by Elliott [17], the growth per cycle is 0.393 monolayers/cycle. The growth per cycle on the substrate $\Delta\Theta_{\text{Si}} = 0.024$ monolayers/cycle is found by manually fitting the average thickness to the measured XPS data.

The vapor pressure of the various precursors determines the actual pressure in the reaction chamber. The mean free path of the high energy electrons at the pressures used, is smaller than the distance traveled in the reaction chamber. Therefore, the intensity of the signal depends on the changing gas composition in the ALD cycle. However, the purge steps after the H_2O and TMA pulses are identical in pressure and atmosphere, and are used as measurement windows.

Figure 5 shows the measured intensity during the N_2 purge step after each ALD cycle. The line is the result of manually fitting the measured data by changing the growth per cycle values $\Delta\Theta_{\text{Si}}$ and $\Delta\Theta_{\text{AlOx}}$, and scattering factors f_{Si} and f_{AlOx} . The result of the best fits with their sum of squared errors (SSE) can be found in table I.

The deposition of amorphous Al_2O_3 results in the change of electron diffraction pattern to diffuse scattering. An additional variation of intensity is visible during every ALD cycle, before the signal is completely decayed. Figure 6 shows the intensity signal during 3 consecutive ALD cycles.

The two binary signal lines in the top of figure 6 indicate

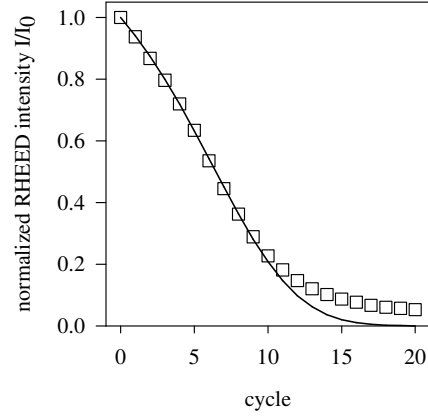


Fig. 5

MODEL FIT (USING EQUATIONS 3 AND 4) OF THE INTENSITY MEASURED DURING THE N_2 PURGE STEP AFTER EACH ALD CYCLE.

	out-of-phase	in-phase
f_{Si}	1	0.97
$\Delta\Theta_{\text{Si}}$	0.025	0.038
f_{AlOx}	0.22	0.22
$\Delta\Theta_{\text{AlOx}}$	0.24	0.29
SSE	$3.1 \cdot 10^{-4}$	$2.4 \cdot 10^{-4}$

TABLE I

MODEL FITTING TO THE MEASUREMENT DATA OF THE FIRST 10 ALD CYCLES AND THE MINIMUM SUM OF SQUARED ERRORS.

the actual valve position of the two precursors. At the start of a purge step (at the closing of precursor valves) a rapid reduction and recovery of the intensity signal is observed. This is due to a high pressure burst of N_2 purge gas, intrinsic to the hardware used, which reduces the mean free path of the electrons.

Figure 7 shows the effect of the reactive pulse (TMA or H_2O) on the intensity, based on the measured values during the purge steps. The change of intensity is calculated relative to the intensity level before exposure to the reactive pulse. Figure 7 also shows the ratio of the intensity changes due to TMA and due to H_2O exposure. This ratio appears to be a constant value after the first ALD cycle. The deviation of the first cycle is an indication of growth inhibition and growth initiation by TMA. [18]

V. DISCUSSION

The intensity calculation in the growth model can be fit to the measured intensity, at least for the first 10 cycles.

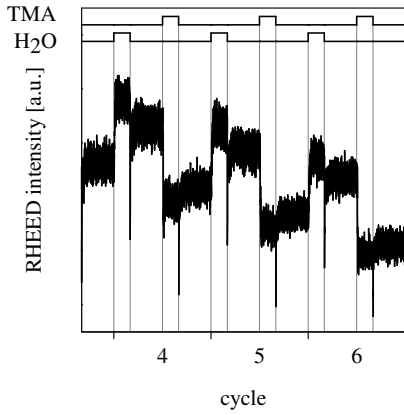


Fig. 6

INTENSITY CHANGE OF THE RHEED SPOT DURING 3 CONSECUTIVE 30 s ALD CYCLES AND ITS RELATION TO THE OPENED/CLOSED (HIGH/LOW) STATUS OF THE PRECURSOR VALVES.

The intensity closely matches the measurement with $\Delta\Theta_{Si} = 0.025$ and $\Delta\Theta_{AlOx} = 0.24$. The only deviation with the measurement is the decay at the end of the process: the model decays beyond the background intensity level of the measurement. The average thickness calculated from the model, is only 1.7 monolayers after 20 cycles. The XPS thickness measurements (and the extracted growth per cycle values) indicate an average thickness of 4.7 monolayers after 20 cycles. This difference can be contributed to process conditions and model accuracy, but also to the formation of the interfacial oxide layer before the start of the RHEED measurement.

The scattering cross section of neutral atoms is related to the electron scattering factor and the atom number. In the deposition of Al_2O_3 from TMA and H_2O , a model system for ALD high- κ oxides, only low numbered (light) atoms are used. Therefore, a change in electron scattering intensity [19] is expected to be not only due to a contribution of deposited aluminum atoms, but also to removal of precursor ligands.

In general, the intensity signal reduces to its noise level in about 20 ALD cycles. The change in signal due to exposure to precursors is not always as strongly visible as in figure 7, even under apparently the same process conditions. This is probably caused by small differences in the angle of incidence of the electron beam. A clear change in intensity of the signal was observed due to exposure to the reactive precursors. The decay in intensity due to (random) deposition of aluminum atoms was expected and will be faster when larger atoms are deposited. In general, the

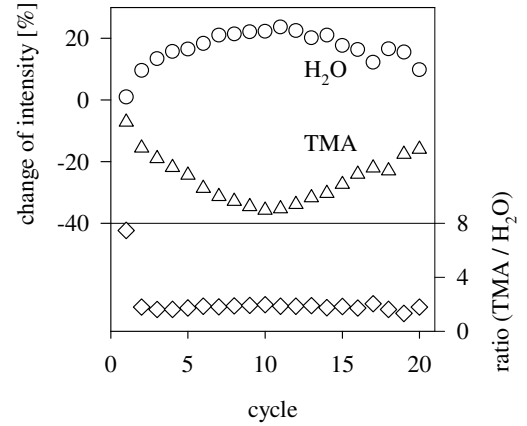


Fig. 7

CHANGE IN RHEED SPOT INTENSITY DUE TO THE REACTIVE PRECURSOR, AS MEASURED DURING THE N_2 PURGE BEFORE AND AFTER THE PRECURSOR PULSE. ALSO, THE RATIO OF CHANGES IN RHEED INTENSITY DUE TO TMA AND DUE TO H_2O EXPOSURE (TMA/ H_2O).

reduction in reflected intensity is related to an increase in surface roughness. The recovery of intensity due to exposure to H_2O is contributed to the removal of the methyl ligands, which is actually a reduction of surface roughness. The new hydroxylated bonding sites have a lower scattering power than the removed methyl groups.

Of all ALD cycles j , the odd and even cycles could be used to model exposure to TMA with scattering factor f_{TMA} and exposure to H_2O with scattering factor f_{H_2O} , respectively. The change from modeling growth per cycle to modeling the exposure to each precursor, requires a modification to the growth model. Sequential exposure to the same precursor, without intermediate exposure to the second precursor, does not result in growth in the ALD chemistry. The ratio between scattering factors for TMA and H_2O is expected to be related to the measured ratio of change in intensity in figure 7. Although the model is time discrete and calculated as numerical series, fitting to the measurement data by iteration would result in more accurate results.

VI. CONCLUSIONS

We have successfully obtained RHEED signals from a surface during atomic layer deposition of Al_2O_3 on silicon and have presented the feasibility of in-situ RHEED analysis during the ALD process. Combining the information extracted from in-situ RHEED measurements with ALD growth models, could result in model improvements and contribute to the proof of its validity.

ACKNOWLEDGMENT

A.I. Zinine (chair of Solid State Physics, University of Twente) is acknowledged for the XPS thickness measurements, as presented in figure 4.

REFERENCES

- [1] R.L. Puurunen and W. Vandervorst, *J. Appl. Phys.* 96 (2004) 7686.
- [2] H. Nohira et al., *J. Non-Cryst. Solids* 303 (2002) 83.
- [3] R.K. Grubbs, C.E. Nelson, N.J. Steinmetz, S.M. George, *Thin Solid Films* 467 (2004) 16.
- [4] A.J.H.M. Rijnders, G. Koster, D. Blank and H. Rogalla, *Appl. Phys. Lett.* 70 (1997) 1888.
- [5] K. Sawada, M. Ishida and T. Nakamura, *Appl. Phys. Lett.* 52 (1988) 1672.
- [6] K. Kukli, M. Ritala, M. Schuisky, T. Sajavaara, J. Keinonen, T. Uustare and A. Härsta, *Chem. Vapor Depos.* 6 (2000) 303.
- [7] A. Tarre, A. Rosental, V. Sammelseg and T. Uustare, *Appl. Surf. Sci.* 175-176 (2001) 111.
- [8] J.J. Senkevich, F. Tang, D. Rogers, J.T. Drotar, C. Jezewski, W.A. Lanford, G.-C. Wang and T.-M. Lu, *Chem. Vapor Depos.* 9 (2003) 258.
- [9] W. Braun, *Applied RHEED* (Springer, Berlin, 1999).
- [10] J.M. van Hove, C.S. Lent, P.R. Pukite and P.I. Cohen, *J. Vac. Sci. Technol. B* 1 (1983) 741.
- [11] Z.L. Wang, *Reflection electron microscopy and spectroscopy for surface analysis* (Cambridge University Press, Cambridge, 1996).
- [12] E.W. McDaniel, *Collision phenomena in ionized gases* (John Wiley & Sons, New York, 1964).
- [13] P. Doyle, P.S. Turner, *Acta Crystallogr. A* 24 (1986) 390.
- [14] P.I. Cohen, G.S. Petrich, P.R. Pukite, G.J. Whaley and A.S. Arrott, *Surf. Sci.* 216 (1989) 222.
- [15] R.L. Puurunen, *Chem. Vapor Depos.* 10 (2004) 159.
- [16] J.W. Evans, *Phys. Rev. B* 39 (1989) 5655.
- [17] S.D. Elliott, H.P. Pinto, *J. Electroceramics* 13 (2004) 117.
- [18] M.M. Frank, Y.J. Chabal, G.D. Wilk, *Appl. Phys. Lett.* 82 (2003) 4758.
- [19] H.S.W. Massey, E.H.S. Burhop, H.B. Gilbody, *Electronic and ionic impact phenomena* (Oxford University Press, Oxford, 1969).